

## Six-Center Assessment of CNN-Transformer with Belief Matching Loss for Patient-Independent Seizure Detection in EEG

Peh, Wei Yan; Thangavel, Prasanth; Yao, Yuanyuan ; Thomas, John; Tan, Yee Leng; Dauwels, Justin

**DOI**

[10.1142/S0129065723500120](https://doi.org/10.1142/S0129065723500120)

**Publication date**

2023

**Document Version**

Final published version

**Published in**

International Journal of Neural Systems

**Citation (APA)**

Peh, W. Y., Thangavel, P., Yao, Y., Thomas, J., Tan, Y. L., & Dauwels, J. (2023). Six-Center Assessment of CNN-Transformer with Belief Matching Loss for Patient-Independent Seizure Detection in EEG. *International Journal of Neural Systems*, 33(3), Article 2350012. <https://doi.org/10.1142/S0129065723500120>

**Important note**

To cite this publication, please use the final published version (if applicable). Please check the document version above.

**Copyright**

Other than for strictly personal use, it is not permitted to download, forward or distribute the text or part of it, without the consent of the author(s) and/or copyright holder(s), unless the work is under an open content license such as Creative Commons.

**Takedown policy**

Please contact us and provide details if you believe this document breaches copyrights. We will remove access to the work immediately and investigate your claim.

***Green Open Access added to TU Delft Institutional Repository***

***'You share, we take care!' - Taverne project***

**<https://www.openaccess.nl/en/you-share-we-take-care>**

Otherwise as indicated in the copyright section: the publisher is the copyright holder of this work and the author uses the Dutch legislation to make this work public.

## Six-Center Assessment of CNN-Transformer with Belief Matching Loss for Patient-Independent Seizure Detection in EEG\*

Wei Yan Peh<sup>†</sup>, Prasanth Thangavel<sup>†</sup>, Yuanyuan Yao<sup>‡</sup>, John Thomas<sup>§</sup>,  
Yee-Leng Tan<sup>¶</sup> and Justin Dauwels<sup>||,\*\*</sup>

<sup>†</sup>*Interdisciplinary Graduate School (IGS)*

*Nanyang Technological University, Singapore 639798*

<sup>‡</sup>*Katholieke Universiteit Leuven, Oude Markt 13, 3000 Leuven, Belgium*

<sup>§</sup>*Montreal Neurological Institute, McGill University, Montreal QC H3A 2B4, Canada*

<sup>¶</sup>*National Neuroscience Institute, Singapore 308433*

<sup>||</sup>*Department of Microelectronics, Delft, University of Technology*

*2628 CD Delft, Netherlands*

*\*\*j.h.g.dauwels@tudelft.nl*

Accepted 15 December 2022

Published Online 22 February 2023

Neurologists typically identify epileptic seizures from electroencephalograms (EEGs) by visual inspection. This process is often time-consuming, especially for EEG recordings that last hours or days. To expedite the process, a reliable, automated, and patient-independent seizure detector is essential. However, developing a patient-independent seizure detector is challenging as seizures exhibit diverse characteristics across patients and recording devices. In this study, we propose a patient-independent seizure detector to automatically detect seizures in both scalp EEG and intracranial EEG (iEEG). First, we deploy a convolutional neural network with transformers and belief matching loss to detect seizures in single-channel EEG segments. Next, we extract regional features from the channel-level outputs to detect seizures in multi-channel EEG segments. At last, we apply post-processing filters to the segment-level outputs to determine seizures' start and end points in multi-channel EEGs. Finally, we introduce the minimum overlap evaluation scoring as an evaluation metric that accounts for minimum overlap between the detection and seizure, improving upon existing assessment metrics. We trained the seizure detector on the Temple University Hospital Seizure (TUH-SZ) dataset and evaluated it on five independent EEG datasets. We evaluate the systems with the following metrics: sensitivity (SEN), precision (PRE), and average and median false positive rate per hour (aFPR/h and mFPR/h). Across four adult scalp EEG and iEEG datasets, we obtained SEN of 0.617–1.00, PRE of 0.534–1.00, aFPR/h of 0.425–2.002, and mFPR/h of 0–1.003. The proposed seizure detector can detect seizures in adult EEGs and takes less than 15 s for a 30 min EEG. Hence, this system could aid clinicians in reliably identifying seizures expeditiously, allocating more time for devising proper treatment.

*Keywords:* Transformer; belief matching; electroencephalogram; patient-independent seizure detection.

\* An extended version of this paper can be found in <https://arXiv.org/abs/2208.00025>.

\*\* Corresponding author.

## 1. Introduction

Epilepsy is a brain disorder characterized by the manifestations of sudden unprovoked seizures.<sup>1</sup> Seizures are diverse and vary significantly across patients in etiology, severity, and symptoms.<sup>2</sup> Most electrographic seizures last from 30 s to 2 min, where a seizure lasting longer than 5 min is a medical emergency.<sup>3</sup> Epilepsy is diagnosed when a patient experiences two or more recurring seizures.<sup>4</sup> Around 1% of the world population is diagnosed with epilepsy.<sup>5</sup> Moreover, approximately 10% of the population will experience a seizure within their lifetime.<sup>6</sup> Overall, provoked and unprovoked seizures occur in about 3.5 and 4.2 per 10,000 individuals annually, respectively.<sup>5</sup> After a seizure episode, the likelihood of encountering another seizure event increases to about 50%, bringing the individual to a much greater risk of relapsing.<sup>7</sup>

To detect seizures, an electroencephalogram (EEG) can be utilized to measure the electrical activity in the brain.<sup>5</sup> Scalp EEG records the brain activity with surface electrodes, while intracranial EEG (iEEG) measures the signals directly via implanted electrodes.<sup>8</sup> However, visual inspection of EEGs can be time-consuming.<sup>9</sup> There is a need for automated detectors that can detect seizures reliably and quickly. Most progress has been made toward patient-specific detectors, as seizure morphologies vary across patients. Consequently, designing a seizure detector that can detect seizures in any patient can be challenging but tremendously helpful for clinicians.

In recent studies on automated seizure detection from EEG, the detectors are validated mainly on two public seizure datasets: the Temple University Hospital seizure (TUH-SZ) dataset<sup>10–12</sup> and the Children’s Hospital Boston Massachusetts Institute of Technology (CHB-MIT) dataset.<sup>11,13–15</sup> In many studies, different models are proposed, including wavelet analysis,<sup>16–18</sup> machine learning models,<sup>19</sup> convolutional neural networks (CNNs),<sup>10,12,13,15,20</sup> recurrent neural networks (RNNs),<sup>10</sup> long short-term memory (LSTM),<sup>21</sup> transformer,<sup>22</sup> transfer learning,<sup>23–26</sup> quickest detection,<sup>27</sup> and temporal graph convolutional networks (TGCNs).<sup>28</sup>

The seizure detectors proposed in these studies are similar in architecture and/or implementation. The detectors first divide the EEGs into

short multi-channel segments (segment-level), before classifying each segment as normal against seizure. Then, using the segment-level outputs, they determine the start and end points of the seizures in full EEGs. The main innovation in these studies lies in the design of the segment-level detector, where most studies propose increasingly deep and complex neural networks with millions of parameters.<sup>22,28</sup>

Unfortunately, computationally intensive models may not necessarily improve patient-independent seizure detection due to the increased risk of overfitting.<sup>28,29</sup> Furthermore, detectors trained on larger datasets had reported similar results to those trained on smaller datasets.<sup>28,30</sup> For instance, Covert *et al.*<sup>28</sup> had used a vastly larger dataset than Yuan *et al.*<sup>30</sup> (18741 EEGs versus 686 EEGs, respectively); yet, they obtained similar if not poorer results than Yuan *et al.* (AUC of 0.935 versus 0.967, respectively). While we acknowledge possible differences between the quality and type of EEG used in both studies, using more data does not seem to help improve the seizure detection problem.

To resolve the bottleneck, we require a fresh perspective on this problem. As we will explain in the following, we address certain drawbacks of existing seizure detectors and resolve some of their weaknesses in this study.

First, most modern seizure detectors identify seizures at the segment-level directly. Since these detectors are trained on multi-channel EEG segments, they can only handle a fixed number of EEG electrodes (e.g. 21). To apply those models to EEGs with a different number of electrodes (32), the models need to be retrained. In practice, the number of electrodes may vary, and this limitation is a severe impediment to clinical applications.

To overcome this, we proposed a seizure detector that starts by detecting seizures in single-channel segments (channel-level detection). We evaluate three variations of CNN for the channel-level detector: CNN with softmax loss (CNN-SM), CNN with belief matching (BM) loss (CNN-BM), and a CNN cascaded with a transformer and BM loss (CNN-TRF-BM). The BM loss is used to improve calibration performance. It does so by trying to model the distribution and behavior of the probability predicted to be similar to the distribution and behavior of probability observed in training data.<sup>31</sup>

Hence, calibration improves the probability estimate of a data point belonging to a class. Meanwhile, the transformer is deployed to extract long-range patterns across the signals via self-attention, which the CNNs cannot. Several existing studies have proposed systems to detect seizures at the channel-level.<sup>32–34</sup> However, some of these only analyzed single-channel EEGs instead of multi-channel EEGs.<sup>32</sup> Consequently, they do not consider segment-level detection, in contrast to the study at hand.

To resolve the restriction on the fixed number of channels, we aggregate the channel-level outputs and group them into five distinct brain regions. Then, we compute statistical features from each region, which can be done for an arbitrary number of electrodes. This approach allows us to apply the detectors to EEGs with any number of electrodes and both scalp EEG and iEEGs. In this study, we trained the proposed seizure detector on a large scalp EEG dataset (TUH-SZ dataset) and evaluated it on five independent scalp EEG and iEEG datasets. In contrast, few research studies investigate both scalp EEG and iEEG together. Moreover, for seizure detectors evaluated on both scalp EEG and iEEG, those detectors are often trained and analyzed separately.<sup>22,35</sup>

Finally, a good evaluation metric to measure the effectiveness of seizure detectors is necessary. Such metrics score a detection from the automated system based on how much it overlaps with a manually annotated seizure(s). For channel- or segment-level EEG seizure detection, the problem is binary: ictal versus nonictal. Consequently, standard metrics for binary classification are applied in the literature for channel- or segment-level EEG seizure detection. However, EEG-level seizure detection, particularly event-based seizure detection, is more complicated. In this scenario, the problem is no longer a binary classification problem. Instead, the problem is to determine whether a detection had correctly detected a seizure based on the overlap between the detection and the seizure(s). Unfortunately, most studies use different evaluation approaches to assess the detectors, making comparison studies challenging. Several evaluation metrics have been proposed, including epoch-based sampling (EBS),<sup>36</sup> any-overlap (OVLP),<sup>36</sup> time-aligned event scoring (TAES),<sup>36</sup> and increased margin scoring (IMS).<sup>37</sup> However, these metrics do not reflect real-world clinical requirements.

For instance, Reus *et al.*<sup>37</sup> only reported IMS, which considers a detection correct as long as the detection is within 30s before the start or after the end of the seizure, respectively. Similarly, Koren *et al.*<sup>38</sup> reported IMS, and increased the time margin to 120s. Allowing this significant error margin could lead to huge uncertainty and low precision (PRE) during detection. Meanwhile, Fürbass *et al.*<sup>13</sup> determine that a seizure is detected as long as a detection appears within a seizure event. These approaches ignored the amount of overlap required, making their measurement approach extremely lenient. Either way, it is inappropriate in clinical practice.

Therefore, we introduce the minimum overlap evaluation scoring (MOES), which requires the detection from the automated system to have a minimum overlap duration of 10s and a minimum overlap of 30% with a ground truth seizure for it to be considered correct. In contrast, OVLP and TAES require a nonzero (e.g. 0.1%) and perfect (100%) overlap, respectively, which tends to under- or over-penalize the detector. By requiring a nontrivial overlap, albeit not necessarily a perfect overlap, the MOES metric has an adequate tolerance for clinical practice.

In summary, this paper performs the following:

- (1) We developed a patient-independent seizure detector that can be applied to scalp EEG and iEEG, regardless of the number of electrodes.
- (2) We utilize a BM loss to improve the calibration performance, which is critical for decision-making. However, such approaches are rarely applied in EEG analysis, as most studies favor softmax (SM) loss. Unfortunately, many existing classification algorithms are not optimized for obtaining accurate probabilities, and their predictions may be miscalibrated.
- (3) We apply CNN with transformers as a transformer can extract long-range patterns, which a CNN cannot. Transformers had been explored for seizure detection (see Ref. 22) but have yet to be applied at the channel-level.
- (4) We train the proposed detector on one scalp EEG dataset and test it on five independent scalp EEG and iEEG datasets. Seizure detectors are usually not assessed simultaneously on multiple datasets and not on scalp EEGs and iEEGs.

- (5) We introduce the MOES to assess the performance of seizure detectors. In contrast to existing metrics, the MOES metric requires a nontrivial but not necessarily perfect overlap between the detection and ground truth seizure(s) for the detection to be considered correct. Existing metrics are too lenient or strict on the overlap criteria, resulting in inaccurate results.

## 2. Materials and Methods

### 2.1. Dataset

We analyze six public EEG datasets in this study:

- (1) Temple University Hospital Seizure (TUH-SZ) dataset<sup>39</sup>
- (2) Children’s Hospital Boston Massachusetts Institute of Technology (CHB-MIT) dataset<sup>40</sup>
- (3) Helsinki University Hospital (HUH) dataset<sup>41</sup>
- (4) Sleep Wake Epilepsy Center at ETH Zurich (SWEC-ETHZ) dataset<sup>42</sup>
- (5) International Epilepsy Electrophysiology Portal (IEEGP) dataset<sup>43</sup>
- (6) Epilepsy iEEG Multicenter (EIM) dataset.<sup>44</sup>

Information about the six datasets is summarized in Table 1. The TUH-SZ dataset is the largest among those six datasets, with the most annotated seizure events. Hence, we utilized the TUH-SZ dataset as the primary source to train the entire seizure detector pipeline.

First, the seizure detector is trained and evaluated with the TUH-SZ dataset via four-fold cross-

validation (CV). We assign approximately the same number of patients and seizures to each fold. Next, using the trained detector, we further assess it on five other independent EEG datasets. In this way, we examine the generalizability of the detector on different EEG datasets with different EEG types and patient age groups.

For all the EEGs, a fourth-order Butterworth notch filter at 60 Hz (USA) and 50 Hz (EU) is applied to remove electrical interference.<sup>45</sup> Next, a 1 Hz high-pass filter (fourth order) is implemented to reject DC shifts and baseline fluctuations.<sup>46</sup> Finally, all the EEGs are downsampled to a sampling frequency  $F_s$  of 128 Hz. At last, we convert all scalp EEGs to bipolar montage, as the TUH-SZ dataset is annotated in the bipolar montage. As the montage for the iEEGs is incompatible with the bipolar montage, we keep the montage of the iEEGs at monopolar.

### 2.2. Seizure detector pipeline

We perform seizure detection first at individual channels (channel-level detection), followed by multi-channel segments (segment-level detection). At last, we detect the start and end points of the seizures in the entire multi-channel EEG (EEG-level detection)<sup>45–47</sup> (see Fig. 1). The proposed seizure detector is displayed in Fig. 2. The pipeline consists of a channel-level deep learning classifier, a segment-level machine learning classifier, and multiple EEG-level post-processing modules. The seizure detectors are

Table 1. Information on the six scalp EEG and iEEG datasets analyzed in the study.

Information	Details	TUH-SZ	CHB-MIT	HUH	SWEC-ETHZ	IEEGP	EIM
EEG Details	Patient Type	Human	Human	Human	Human	Human/Dog	Human
	Patient Age Group	Adult	Paediatric	Neonatal	Adult	Adult	Adult
	EEG Type	scalp EEG	scalp EEG	scalp EEG	iEEG	iEEG	iEEG
	$F_s$ (Hz)	250-1000	256	256	512	400-5000	250-1000
	Channel Name	Available	Available	Available	Unavailable	Unavailable	Unavailable
	Channel-level Annotation	Yes	No	No	No	No	No
	Seizure Label, Type	Yes, 8	No	No	No	No	No
	No of Channels	19,21	23,24,26	21	36–100	16–72	53–216
Number of Patients and EEGs	Patients	637	24	75	16	12	31
	All EEGs	5,610	683	75	100	12	102
	Non-Seizure EEGs	4,450	545	22	0	0	0
	Seizure EEGs	1,150	138	54	100	12	102
	Seizure Events	3,050	185	517	100	12	102
Duration	All EEGs (in hours)	922	980	114	13.5	7.20	7.96
	Non-SZ EEGs (in hours)	681	792	35.0	0	0	0
	SZ EEGs (in hours)	242	188	78.6	13.5	7.20	7.96
	Average (All) (in minutes)	9.84	86.1	89.64	8.1	36	4.68
	Average SZ (in seconds)	54.3	54.4	90.5	95.9	37.3	103.7

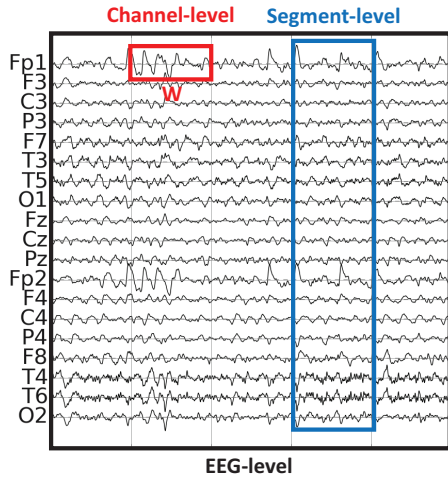


Fig. 1. The three EEG scales: channel-, segment-, and EEG-level detection.

implemented on NVIDIA GeForce GTX1080 GPUs in Keras 2.2.0 and TensorFlow 2.6.0.

### 2.3. Channel-level seizure detector

The channel-level seizure detector computes the seizure probability for single-channel EEG segments. The window length  $W$  adopted in the literature

ranges between 1s to 30s. However,  $W = 1$  s is too short to capture long-range seizure morphology, while  $W = 30$  s is too long to capture short seizures. Therefore, we tested window lengths  $W \in \{3, 5, 10, 20\}$  s. In this study, we deploy three channel-level seizure detectors based on CNNs:

- (1) CNN with softmax (SM) loss: CNN-SM.
- (2) CNN with belief matching (BM) loss: CNN-BM.
- (3) CNN-transformer with BM loss: CNN-TRF-BM.

#### 2.3.1. CNN-SM model

The CNN-SM model is a CNN with a SM loss function. The input is the raw single-channel signal of length  $W \times F_s$ . The architecture contains five convolutional layers with 8, 16, 32, 64, and 128 filters, respectively, with two fully connected layers. To minimize the loss, we applied the Adam optimizer with an initial learning rate equal to  $10^{-4}$ . The batch size during training is set to 1000. Also, we implemented class weights that are inversely proportional to the class frequency in the training data during training. This allows us to optimize the loss function on an imbalanced dataset without overfitting.<sup>47</sup> Finally, we optimized parameters within the CNN via nested CV

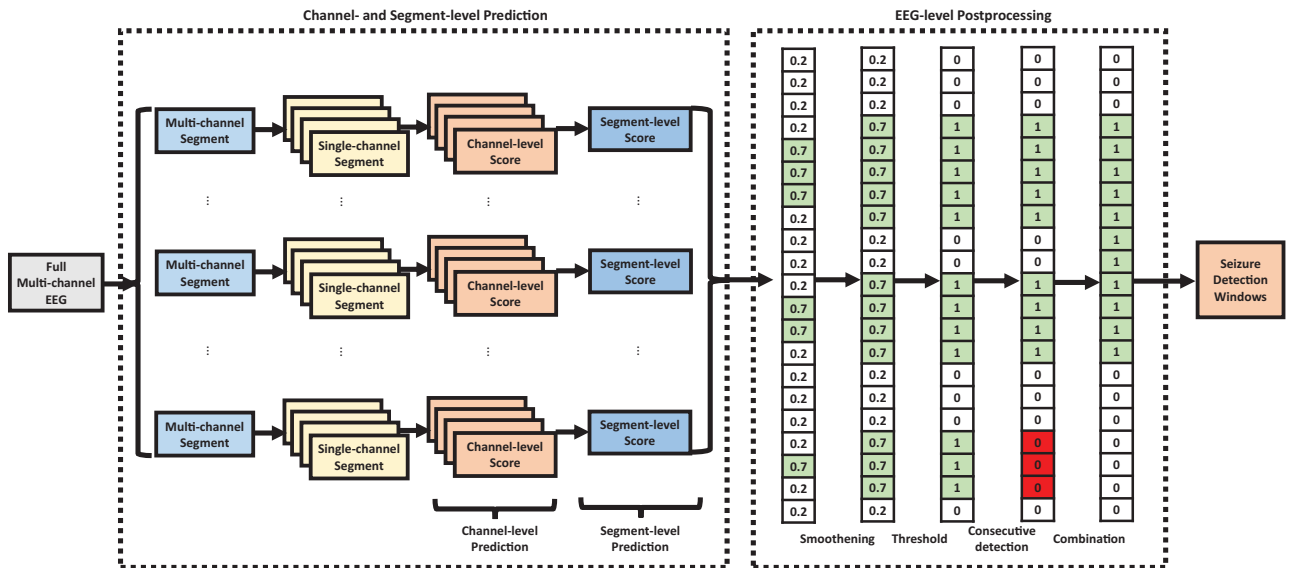


Fig. 2. The proposed seizure detector pipeline consists of multiple stages of seizure detection at three EEG scales. The EEG is divided into overlapping epochs where we performed channel- and segment-level detection to get a series of segment-level outputs. Next, we applied four post-processing steps for EEG-level detection. First, we apply smoothing window (e.g. max smoothen window of length 3) to the segment-level output. Second, we implement thresholds (e.g. 0.5) to obtain a series of 0s and 1s. Third, we locate chains of consecutive 1s and replace them with 0s if the chain is less than  $N_c$  (e.g.  $N_c = 4$ ) in length. Finally, suppose any two chains of consecutive 1s are within proximity (e.g. 3 epochs). In that case, we combine them into a single detection to prevent many fractured detection windows.

on the training data, with an 80:20% split for training and validation.

### 2.3.2. CNN-BM model

The CNN-BM model has the same architecture as the CNN-SM model, except that the BM loss replaces the SM loss. The BM loss is shown to yield better uncertainty estimates and generalization performance than the SM loss, an important property required for seizure detection.<sup>48</sup> The BM framework is formulated from a Bayesian perspective that views binary classification as distribution matching. The BM loss is defined as

$$\mathcal{L}(\mathbf{W}) \approx -\frac{1}{m} \sum_{i=1}^m \ell_{\text{EB}}(y^{(i)}, \alpha^{\mathbf{W}}(\mathbf{x}^{(i)})), \quad (1)$$

where  $\mathbf{x}^{(i)}$  and  $y^{(i)}$  is the  $i$ th training data and its label, respectively,  $m$  is the total number of samples, and  $\alpha^{\mathbf{W}} = \exp(\mathbf{W})$ , where  $\mathbf{W}$  are the weights of the neural network classifier.  $\ell_{\text{EB}}(y, \alpha^{\mathbf{W}}(\mathbf{x}))$  is the evidence lower bound (ELBO)<sup>48</sup> and is defined as  $\ell_{\text{EB}}(y, \alpha^{\mathbf{W}}(\mathbf{x})) = \mathbb{E}_{q_{\mathbf{z}|\mathbf{x}}^{\mathbf{W}}}[\log p(y|\mathbf{x}, \mathbf{z})] - \text{KL}(q_{\mathbf{z}|\mathbf{x}}^{\mathbf{W}} \| p_{\mathbf{z}|\mathbf{x}})$ , where  $\mathbf{z}$  is the categorical probability about the label,  $p_{\mathbf{z}|\mathbf{x}}$  is the target distribution,  $q_{\mathbf{z}|\mathbf{x}}^{\mathbf{W}}$  is the approximate distribution, and KL is the KL-divergence. We refer to Ref. 48 for more information on the BM loss.

### 2.3.3. CNN-TRF-BM model

The CNN-TRF-BM model contains the CNN and the transformer. The architecture is the same as in the CNN-BM model, but we insert an additional transformer encoder between the final convolutional layer and the flattening layer (see Ref. 49). We implemented a transformer in tandem with the CNN, as the CNN alone cannot model correlations between distant data points, such as seizure morphologies. The transformer can compensate for this limitation by extracting long-range information from the CNN features. The transformer encoder contains eight heads, and the number of hidden layer neurons in the forward feed network (FFN) is 1024. As input to the transformer, we extract 1s segments with 25% overlap from the  $W$ -second single-channel segment.

## 2.4. Segment-level seizure detector

Next, we rely on the outputs of the channel-level detectors to detect seizures in multi-channel segments. The channel-level detectors yield seizure probabilities for each EEG channel, which we arrange into regions according to the scalp topology: frontal, central, occipital, and parietal. Besides those four local regions, we also define a ‘‘global’’ region containing all channels. From each region, we extract seven statistical features: mean, median, standard deviation, maximum value, minimum value, and value at 25% and 75% percentile. As there are five regions, we extract  $5 \times 7 = 35$  features. From all channel-level outputs, we compute the normalized histogram features (5 bins, range [0, 1]) and include them into the feature set, bringing the total features to 40.

In the iEEGs, the channel locations are unavailable; hence we cannot group the iEEG channels into local regions. Instead, we replace the four local regions with the global region. In this scenario, only 12 features are unique, and the remaining ones are duplicates. In any case, the number of segment-level features is 40, regardless of the number of channels or the availability of the channel locations. This approach ensures that the number of features is consistent during the training and evaluation of any dataset. The features will be the inputs to an XGBoost model for training and validation, and we determined the hyperparameters via grid search CV. We selected the XGBoost model, as it is a state-of-the-art machine learning model that outperforms most classical models such as the support vector machine (SVM) and random forest.<sup>50</sup>

## 2.5. Channel- and segment-level evaluation metric

We assess the channel- and segment-level seizure classifiers through the following metrics: accuracy (ACC), balanced accuracy (BAC), sensitivity (SEN), specificity (SPE), F1 score (F1), and expected calibration error (ECE).<sup>31</sup> As the seizure and non-seizure classes are imbalanced, we evaluate the results mainly in BAC.<sup>47</sup>

## 2.6. EEG-level seizure detector

Finally, we perform seizure detection on full EEGs by determining the start and end time of the seizures,



if any. First, we apply a sliding window of length  $W$  with a shift duration  $T_o$  to the multi-channel EEG, extracting  $n$  multi-channel segments. Here,  $n$  depends on the duration of the EEG recording. If the EEG recording lasts only 20 s,  $n = 1$ . However, if the EEG recording is 3600 s,  $n = \frac{3600-20}{1} + 1 = 3581$ . The overlap duration  $T_o$  is set to 1 s. Next, we perform segment-level detection on each segment, resulting in  $n$  seizure probabilities  $P = [p_1, \dots, p_n]$ . Finally, we conduct three post-processing steps to the seizure probability sequence  $P$ :

- (1) We apply 1D smoothing filters with an overlap of 1 sample. We tested various filter lengths  $K_f$  (3, 5, or 7 s) and filter types (mean, median, or max). The smoothing filter removes isolated seizure detections (usually false positives (FPs) such as artifacts) and smoothens regions with significant confidence variations to stabilize the detections.
- (2) Next, we perform thresholding to the seizure probabilities to round them to zeros (seizure-free) or ones (seizure). We tested threshold values  $\theta \in \{0.1, 0.2, \dots, 0.8, 0.9\}$ .
- (3) Then, we identify consecutive ones of length smaller than  $N_c$ , and replace the 1s with 0s. Selecting a large  $N_c$  removes many short detections, leading to fewer FPs and more FNs, as the system may miss short seizures. We tested  $N_c \in \{1, 2, \dots, 19, 20\}$ .

Finally, we identify the remaining sequences of consecutive 1s, and determine their start and end time. The final output of the EEG-level seizure detector is the start and end times of the detected seizures.

### 2.7. EEG-level seizure detection evaluation metric

We assess the ACC of the detections via EEG-level seizure detection evaluation metric. There are several well-established evaluation metrics, such as EBS,<sup>36</sup> any-overlap (OVL),<sup>36</sup> TAES,<sup>36</sup> and IMS.<sup>37</sup> However, these metrics do not accurately reflect the clinical requirement of a seizure detector. Hence, we define a new metric, the MOES. In this metric, there needs to be a nontrivial overlap between the detection and the seizure, while it does not need to be perfect.

### 2.8. Minimum overlap evaluation scoring (MOES)

The MOES determines the overlap duration  $T_{\text{overlap}}$  between the detection ( $T_{\text{detection}} = [d_{\text{start}}, d_{\text{end}}]$ ) and seizure ( $T_{\text{seizure}} = [s_{\text{start}}, s_{\text{end}}]$ ) window, and vice versa, before deciding if the detection is correct or the seizure is captured. Based on existing literature, only seizures of at least 10 s are annotated typically.<sup>51</sup> Therefore, the minimum overlap duration of the detection (s) with the seizure should be 10 s. However, these criteria do not account for the duration of the seizure or the detection. Therefore, even if the detection correctly detected over 10 s of a seizure, the system should be penalized if the majority of the detection did not capture any seizure. To resolve this, we compute the detection overlap (DOL) and the seizure overlap (SOL), which measures the fraction of the detection that overlaps with any seizures, and vice versa, as

$$\text{DOL}_i = \frac{\sum_s T_{\text{overlap},s,i}}{d_{\text{end},i} - d_{\text{start},i}}, \quad (2)$$

$$\text{SOL}_j = \frac{\sum_d T_{\text{overlap},d,j}}{s_{\text{end},j} - s_{\text{start},j}}, \quad (3)$$

where  $i$  and  $j$  are the index of a detection and a seizure, respectively,  $\sum_s T_{\text{overlap},s,i}$  is the sum of all the overlaps with any seizures with detection  $i$ , and  $\sum_d T_{\text{overlap},d,j}$  is the sum of all the overlaps with any seizures with seizure  $j$ .

In this study, we set a minimum DOL and SOL of 0.3 (30%) to ensure that a significant portion of the DOLs with the seizures and vice versa. In OVL metric, the DOL is set to be 0+%, while in TAES it is 100%. The first option is too lenient in practice, while the latter is too strict.

A high DOL implies that the DOLs well with the seizure(s). Meanwhile, a high SOL indicates that the seizure is well captured by the detection(s). If the DOL is low, the detection should be discarded and treated as a FP. Similarly, if the SOL is low, the seizure should be treated as a false negative (FN). More details on how MOES approaches different detection cases are elaborated in the extended version of the paper.

Finally, the detection may start earlier or later than the annotated seizure. We compute the detection offset as

$$T_{\text{offset}} = d_{\text{start}} - s_{\text{start}} + W, \quad (4)$$

where  $W$  is the duration of the window length,  $d_{\text{start}}$  is the start time of the detection,  $s_{\text{start}}$  is the start time of the annotated seizure. We added  $W$  in the offset as we require a minimum window of length  $W$  to detect seizures. To more accurately detect the onset of a seizure, one may slide the window in smaller steps around the onset of a detection. However, this goes beyond the scope of this work, as we are mainly interested in detecting seizures, irrespective of their onset times.

### 2.9. EEG-level seizure detection performance metrics

We measure the performance of EEG-level seizure detection with SEN, PRE, false positive per hour (FPR/h), and the offset. All these metrics are essential to provide a fair assessment of the proposed pipeline as an assistive tool for clinical applications. We compute the SEN, PRE, and FPR/h per EEG, before computing their mean values across each dataset. Meanwhile, for FPR/h, we compute the average FPR/h (aFPR/h) and the median FPR/h (mFPR/h).

## 3. Results

### 3.1. Channel-level seizure detection

We performed channel-level seizure detection with three channel-level detectors: CNN-SM, CNN-BM, and CNN-TRF-BM. We summarized the results in Table 2. In addition, all the precision-recall (PR) curves can be found in Fig. 3.

On the TUH-SZ dataset, the proposed channel-level detectors achieve high BAC, SEN, and SPE across all window lengths. Moreover, the ECE improved for all window lengths (except for 3 s) when the SM loss is replaced with the BM loss (CNN-SM against CNN-BM). However, the ECE is slightly larger for the CNN-TRF-BM model. The performance peaks at  $W = 20$  s for all three models. Overall, the CNN-TRF-BM model attained the best results, followed by the CNN-BM and the CNN-SM model. As the channel-level detector attains good results on the TUH-SZ dataset, using it as the primary training dataset seems promising.

Next, we assessed the channel-level detector, trained on the TUH-SZ dataset, on the five EEG datasets. The detectors achieve high BACs on the CHB-MIT, SWEC-ETHZ, and EIM datasets, but

yield poor BACs on the HUH and IEEGP datasets. For those datasets, seizures have only been annotated on the level of segments instead of channels; therefore, it is impossible to assess the channel detector reliably. Without channel-level annotations, we must assume that all channels within a multi-channel segment contain seizures. However, this is unlikely as seizures sometimes only occur in certain regions. In particular, focal seizures occur only in one hemisphere or at a few electrodes. Consequently, channels that do not exhibit seizures may be mislabeled as “seizures”, leading to errors during training and testing. However, segment-level and EEG-level detection results are reliable for those datasets.

### 3.2. Segment-level seizure detection

Next, we performed segment-level seizure detection using the outputs from the three channel-level detectors. The segment-level detection results on the six EEG datasets are displayed in Table 3.

On the TUH-SZ dataset, the proposed segment-level detectors achieve high BAC, SEN, and SPE across all window lengths, similarly to the channel-level results. However, the ECE reported at the segment-level is much greater than the channel-level counterparts, as the segment-level detector model does not minimize ECE. Similarly, the performance peaks at  $W = 20$  s. Again, the CNN-TRF-BM model outshines the other two models.

Next, we evaluated the segment-level seizure detector on the other five datasets. We obtained excellent performance on all the datasets at various window lengths, except for the HUH dataset. The segment-level detectors obtain high BACs on the IEEGP dataset, even when the channel-level results on this dataset are not satisfactory.

Overall, the performance peaks at different window lengths across the six datasets. This might be due to the discrepancy in seizure types, patient types, and patient age groups across the different datasets. For instance, for datasets with many short seizures, one should deploy a window length of 3 s as it can capture shorter seizures, while a window length of 20 s would be suboptimal.

### 3.3. EEG-level seizure detection

Next, we performed EEG-level seizure detection based on the outputs of the segment-level detector.

Table 2. Channel-level seizure detection results for different CNN models across six EEG datasets.

Dataset	W	CNN-SM						CNN-BM						CNN-TRF-BM					
		ECE	ACC	BAC	SEN	SPE	F1	ECE	ACC	BAC	SEN	SPE	F1	ECE	ACC	BAC	SEN	SPE	F1
TUH-SZ Scalp EEG Adult	3	0.043	0.824	0.832	0.808	0.855	0.827	0.046	0.837	0.842	0.827	0.856	0.839	0.052	0.824	0.832	0.773	0.89	0.826
	5	0.043	0.84	0.836	0.769	0.902	0.84	0.035	0.845	0.842	0.862	0.821	0.848	0.03	0.85	0.83	0.767	0.892	0.849
	10	0.044	0.815	0.826	0.809	0.844	0.821	0.021	0.848	0.844	0.78	0.908	0.848	0.056	0.772	0.76	0.868	0.653	0.758
HUH Scalp EEG Neonatal	3	0.259	0.506	0.491	0.187	0.794	0.454	0.399	0.403	0.403	0.249	0.903	0.496	0.408	0.4	0.4	0.245	0.902	0.492
	5	0.28	0.532	0.511	0.12	0.902	0.445	0.481	0.354	0.354	0.168	0.957	0.423	0.377	0.427	0.427	0.289	0.879	0.526
	10	0.228	0.527	0.507	0.217	0.796	0.482	0.403	0.417	0.417	0.264	0.912	0.511	0.508	0.358	0.358	0.168	0.974	0.423
CHB-MIT Scalp EEG Paediatric	3	0.259	0.617	0.756	0.569	0.942	0.649	0.269	0.568	0.74	0.51	0.97	0.601	0.25	0.582	0.747	0.528	0.966	0.617
	5	0.181	0.669	0.763	0.56	0.966	0.668	0.205	0.62	0.739	0.494	0.984	0.616	0.095	0.742	0.808	0.666	0.95	0.755
	10	0.126	0.786	0.816	0.743	0.889	0.79	0.137	0.724	0.782	0.635	0.928	0.733	0.205	0.663	0.748	0.515	0.981	0.649
SWEC-ETHZ iEEG Adult	3	0.069	0.803	0.721	0.56	0.882	0.804	0.127	0.814	0.725	0.557	0.892	0.813	0.107	0.814	0.726	0.56	0.891	0.814
	5	0.066	0.828	0.718	0.502	0.935	0.819	0.108	0.834	0.723	0.514	0.933	0.826	0.097	0.798	0.73	0.614	0.847	0.805
	10	0.084	0.772	0.726	0.648	0.805	0.785	0.112	0.805	0.74	0.628	0.853	0.812	0.094	0.844	0.737	0.535	0.939	0.837
IEEGP iEEG Adult	3	0.358	0.536	0.536	0.453	0.952	0.613	0.346	0.533	0.533	0.444	0.975	0.608	0.351	0.532	0.532	0.445	0.968	0.606
	5	0.417	0.512	0.512	0.416	0.991	0.578	0.398	0.502	0.502	0.404	0.993	0.567	0.317	0.553	0.553	0.473	0.95	0.626
	10	0.317	0.574	0.574	0.508	0.9	0.651	0.352	0.562	0.562	0.479	0.976	0.631	0.386	0.523	0.523	0.428	0.998	0.59
EIM iEEG Adult	3	0.201	0.653	0.662	0.583	0.741	0.643	0.128	0.658	0.669	0.579	0.759	0.649	0.144	0.659	0.666	0.588	0.745	0.651
	5	0.205	0.65	0.684	0.52	0.848	0.633	0.135	0.652	0.687	0.518	0.855	0.638	0.154	0.66	0.653	0.626	0.679	0.653
	10	0.207	0.659	0.641	0.658	0.624	0.65	0.154	0.666	0.663	0.622	0.704	0.66	0.155	0.665	0.701	0.536	0.866	0.653
	20	0.221	0.671	0.703	0.57	0.835	0.662	0.15	0.674	0.695	0.594	0.796	0.669	0.139	0.667	0.716	0.541	0.89	0.658

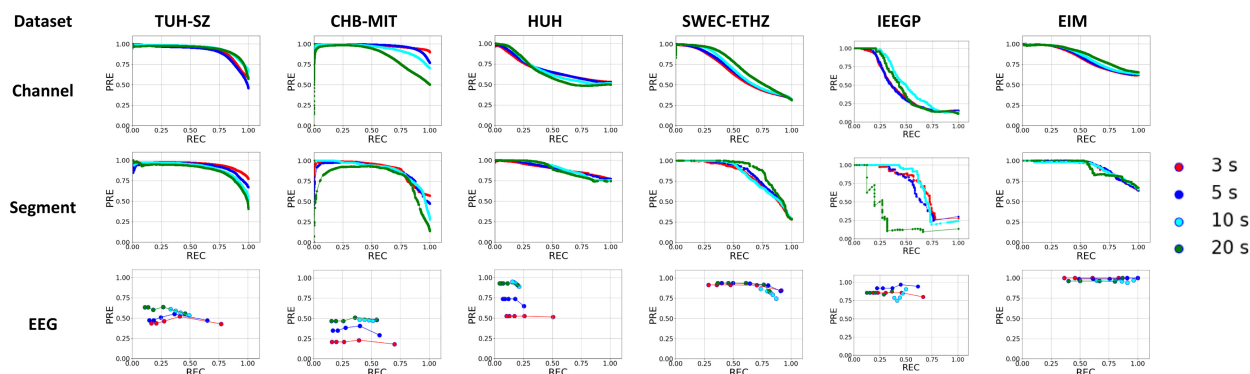


Fig. 3. The precision-recall (PR) curves of the channel-, segment-, and EEG-level seizure detection computed with the CNN-TRF-BM-based seizure detector across different datasets. The EEG-level PR curves are generated by varying the threshold  $\theta$  in the EEG-level postprocessing step and computing the PRE and recall (REC) at each threshold with MOES.

We summarized the results for the six datasets in Table 4. The EEG-level performance is computed according to MOES, as it is more suitable for clinical practice than existing metrics.

On the TUH-SZ dataset, the CNN-TRF-BM model leads to the most promising results, followed by the CNN-BM and the CNN-SM model. The CNN-TRF-BM EEG-level seizure detector attained a respectable SEN, PRE, aFPR/h, mFPR/h, and median offset of 0.772, 0.429, 0.425, 0, and  $-2.125$  s, respectively. While the aFPR/h is high, the mFPR/h is extremely low. This implies that the aFPR/h is skewed by a small number of EEGs containing

an exceptionally huge amount of false detection. While the SEN is similar across all three models, the CNN-TRF-BM model reported the best PRE, which is critical for clinical deployment.

Similarly, we evaluated the EEG-level seizure detectors on the five scalp EEG and iEEG datasets. The CNN models yield high SEN, decent PRE, and low aFPR/h and mFPR/h on the CHB-MIT, SWEC-ETHZ, and EIM datasets. Meanwhile, on the HUH and IEEGP datasets, the model achieves low SEN (0.254 and 0.450, respectively), high PRE (0.841 and 0.917, respectively), and low mFPR/h (0.347 and 0, respectively). The poorer results on

Table 3. Segment-level seizure detection results for different CNN models across six EEG datasets.

Dataset	W	CNN-SM						CNN-BM						CNN-TRF-BM					
		ECE	ACC	BAC	SEN	SPE	F1	ECE	ACC	BAC	SEN	SPE	F1	ECE	ACC	BAC	SEN	SPE	F1
TUH-SZ Scalp EEG Adult	3	0.051	0.818	0.736	0.888	0.584	0.817	0.027	0.820	0.733	0.901	0.565	0.816	0.262	0.823	0.751	0.885	0.616	0.824
	5	0.036	0.804	0.779	0.856	0.702	0.804	0.033	0.810	0.789	0.856	0.722	0.811	0.248	0.814	0.794	0.856	0.732	0.815
	10	0.039	0.815	0.817	0.783	0.850	0.815	0.031	0.833	0.833	0.815	0.852	0.833	0.027	0.832	0.831	0.800	0.862	0.831
	20	0.268	0.833	0.823	0.766	0.881	0.833	0.031	0.841	0.829	0.771	0.888	0.841	0.251	0.856	0.846	0.795	0.897	0.855
HUH Scalp EEG Neonatal	3	0.193	0.514	0.510	0.514	0.507	0.534	0.130	0.776	0.776	0.746	0.926	0.803	0.259	0.614	0.614	0.577	0.735	0.710
	5	0.200	0.470	0.545	0.376	0.714	0.471	0.232	0.746	0.746	0.709	0.932	0.784	0.303	0.533	0.533	0.429	0.869	0.618
	10	0.353	0.407	0.575	0.192	0.957	0.349	0.366	0.651	0.651	0.581	1	0.695	0.467	0.455	0.455	0.292	0.984	0.514
	20	0.357	0.413	0.575	0.183	0.968	0.349	0.414	0.628	0.628	0.533	0.817	0.691	0.444	0.426	0.426	0.251	0.994	0.483
CHB-MIT Scalp EEG Paediatric	3	0.122	0.789	0.801	0.804	0.798	0.789	0.117	0.798	0.811	0.819	0.804	0.801	0.258	0.833	0.847	0.808	0.886	0.837
	5	0.105	0.814	0.824	0.762	0.887	0.808	0.126	0.811	0.816	0.700	0.932	0.808	0.256	0.822	0.824	0.715	0.932	0.819
	10	0.118	0.874	0.841	0.745	0.936	0.867	0.100	0.875	0.831	0.686	0.976	0.862	0.104	0.879	0.837	0.698	0.976	0.866
	20	0.362	0.921	0.838	0.699	0.976	0.910	0.104	0.918	0.815	0.650	0.979	0.906	0.334	0.929	0.847	0.711	0.982	0.920
SWEC-ETHZ iEEG Adult	3	0.285	0.335	0.546	0.981	0.110	0.267	0.532	0.769	0.776	0.808	0.680	0.821	0.278	0.415	0.579	0.959	0.199	0.358
	5	0.487	0.417	0.600	0.980	0.220	0.380	0.355	0.584	0.601	0.514	0.886	0.659	0.234	0.541	0.649	0.917	0.381	0.529
	10	0.231	0.717	0.763	0.871	0.655	0.731	0.131	0.455	0.472	0.311	0.992	0.509	0.196	0.751	0.768	0.841	0.695	0.766
	20	0.226	0.806	0.832	0.881	0.773	0.819	0.151	0.449	0.463	0.296	0.996	0.493	0.261	0.877	0.872	0.858	0.874	0.883
IEEGP iEEG Adult	3	0.289	0.753	0.753	0.727	0.884	0.787	0.308	0.636	0.535	0.952	0.118	0.542	0.376	0.720	0.720	0.769	0.474	0.760
	5	0.311	0.722	0.722	0.779	0.439	0.759	0.278	0.658	0.555	0.968	0.143	0.559	0.325	0.737	0.737	0.706	0.892	0.778
	10	0.306	0.692	0.692	0.631	1	0.738	0.326	0.726	0.679	0.808	0.551	0.697	0.334	0.670	0.670	0.604	1	0.712
	20	0.290	0.621	0.621	0.571	0.720	0.690	0.345	0.757	0.705	0.883	0.528	0.733	0.398	0.616	0.616	0.429	0.991	0.648
EIM iEEG Adult	3	0.292	0.650	0.553	0.953	0.152	0.556	0.180	0.372	0.545	0.939	0.150	0.310	0.201	0.631	0.505	0.999	0.010	0.495
	5	0.279	0.568	0.459	0.893	0.025	0.468	0.280	0.577	0.670	0.904	0.436	0.575	0.203	0.654	0.538	0.989	0.087	0.543
	10	0.262	0.654	0.568	0.909	0.227	0.586	0.224	0.841	0.809	0.785	0.832	0.849	0.218	0.715	0.646	0.926	0.366	0.655
	20	0.204	0.648	0.644	0.603	0.685	0.611	0.246	0.833	0.850	0.886	0.808	0.846	0.224	0.780	0.745	0.881	0.609	0.749

the HUH dataset align with our expectations since it is a neonatal dataset. The morphology of neonatal seizures differs vastly from adult seizures. Since the model has been trained on adult scalp EEG, it struggles to detect seizures in neonatal scalp EEGs. Meanwhile, the IIEGP dataset contains some dog iEEGs, which could have different seizure patterns from adult humans. However, we observed that the detection performance is comparable for human and dog EEGs. Hence, the proposed detector can detect some neonate and dog seizures with high PRE, which can be tremendously valuable.

We also determined the detection offset, defined as the average duration between the start time of the seizure and the start time of its corresponding detection (see Table 4), which can be negative. A negative offset does not imply forecasting, as the EEG data is analyzed offline.<sup>52</sup> Therefore, data from future time intervals are being considered to decide whether an EEG segment is ictal.

Finally, to determine the effectiveness of the CNN-TRF-BM-based EEG-level seizure detector (Fig. 4), we plot the normalized histograms of the TP and FN of seizures detected sorted by event duration, together with the normalized histogram of SEN, PRE, and FPR/h computed from individual EEGs across the datasets. From Fig. 4(a), it can be seen that it is easier to detect a long seizure than

a short event. Figures 4(b) and 4(c) reveal that the SEN and PRE are high for most EEGs, with only a minority of the files having a poor detection rate. Last, Fig. 4(d) confirms that the system does not make false detections in most EEGs, as mFPR/h is 0. Taken together, these figures suggest that the proposed detector performs well across most EEGs.

The proposed seizure detectors, specifically the CNN-TRF-BM-based model, can detect patient-independent seizures at the channel-, segment-, and EEG-level across various scalp EEG and iEEG datasets without retraining. It takes less than 15s computation time to detect seizures in a 30min EEG. Hence, the proposed detector can help automate EEG annotations clinically. However, while the results are appealing for adult human EEG, there is room for improvement for neonatal EEG. One may need to perform additional tuning or retraining to achieve better performance for such cases.

## 4. Discussion

### 4.1. Comparison with existing patient-independent detectors

To compare the proposed seizure detector to the state of the art is challenging, as there is a lack of standardized evaluation metrics, datasets, or training and testing procedures for the problem of seizure

Table 4. EEG-level seizure detection results for different models evaluated with MOES across six EEG datasets.

Dataset	W	CNN-SM					CNN-BM					CNN-Transformer-BM				
		SEN	PRE	aFPR/h	mFPR/h	Offset	SEN	PRE	aFPR/h	mFPR/h	Offset	SEN	PRE	aFPR/h	mFPR/h	Offset
TUH-SZ Scalp EEG Adult	3	0.7	0.457	0.803	0	-4.125	0.713	0.49	0.479	0	-4.5	0.772	0.429	0.425	0	-2.125
	5	0.704	0.48	0.555	0	-4.5	0.701	0.491	0.413	0	-1.5	0.653	0.476	0.411	0	0.625
	10	0.719	0.495	0.466	0	-1	0.701	0.512	0.237	0	1.5	0.671	0.534	0.954	0	0.5
	20	0.707	0.467	0.679	0	6.25	0.708	0.49	0.468	0	6	0.655	0.52	1.037	0	2.875
CHB-MIT Scalp EEG Pediatric	3	0.638	0.112	1.721	1.099	0.711	0.613	0.14	0.916	0.539	-2.763	0.7	0.181	1.095	0.616	0.053
	5	0.678	0.143	1.514	0.868	-4.474	0.568	0.235	0.600	0.158	2.947	0.571	0.292	0.541	0.224	1.605
	10	0.734	0.254	1.041	0.618	0.158	0.704	0.411	0.291	0.026	4.737	0.678	0.377	0.421	0.118	4.684
	20	0.803	0.194	1.224	0.592	6.842	0.741	0.244	0.884	0.368	5.237	0.769	0.383	0.445	0.145	1.474
HUH Scalp EEG Neonatal	3	0.298	0.334	2.565	1.094	6	0.623	0.576	2.320	2.276	-3.52	0.515	0.522	2.874	2.843	-2.255
	5	0.328	0.372	2.413	0.849	4.25	0.314	0.505	1.977	1.933	3.892	0.253	0.649	0.678	0.623	5.098
	10	0.254	0.397	1.671	0.181	11.5	0.214	0.807	0.334	0.303	13.52	0.227	0.818	0.253	0.223	10.853
	20	0.276	0.473	1.340	0.186	14.25	0.283	0.686	0.708	0.674	16.333	0.254	0.841	0.374	0.247	15.245
SWEC-ETHZ iEEG Adult	3	0.743	0.758	2.316	1.415	10.781	0.933	0.865	1.286	0.469	-2.156	0.938	0.878	0.895	0.559	7.687
	5	0.938	0.949	0.362	0	3.781	0.923	0.752	2.854	2.391	0.312	0.933	0.834	1.784	1.127	4.906
	10	0.933	0.785	2.223	0.884	4.187	0.825	0.695	3.265	2.858	15.719	0.857	0.748	2.899	1.648	10.375
	20	0.567	0.711	3.897	3.601	14.937	0.911	0.744	2.764	1.259	16.531	0.849	0.727	3.010	2.205	12.5
IEEGP iEEG Adult	3	0.6	0.964	0.523	0	-19	0.583	0.958	0.500	0	-14.5	0.667	0.8	2.200	2	-19
	5	0.667	0.8	2.624	2	-17	0.583	0.906	1.595	0	-17	0.617	0.944	1.120	0	-17
	10	0.592	0.946	0.750	0	-12	0.45	0.678	5.596	7	-12	0.5	0.753	4.423	5	-12
	20	0.567	0.805	3.846	0	-2	0.542	0.906	1.500	0	-2	0.45	0.917	0.500	0	-2
EIM iEEG Adult	3	0.972	1	0	0	-22.083	0.792	0.904	1.245	1.286	-7	1	1	1.523	0	-32.083
	5	0.979	0.938	1.080	0	-30.083	1	0.972	0.484	0.452	-15.417	1	1	0.647	0	-23.958
	10	1	1	0	0	-23.417	0.931	0.979	0.520	0	10.542	0.931	1	0.830	0	-1.333
	20	0.875	0.964	0.494	0.711	5.208	1	1	0	0	-0.792	0.951	1	0.507	0	-3.125

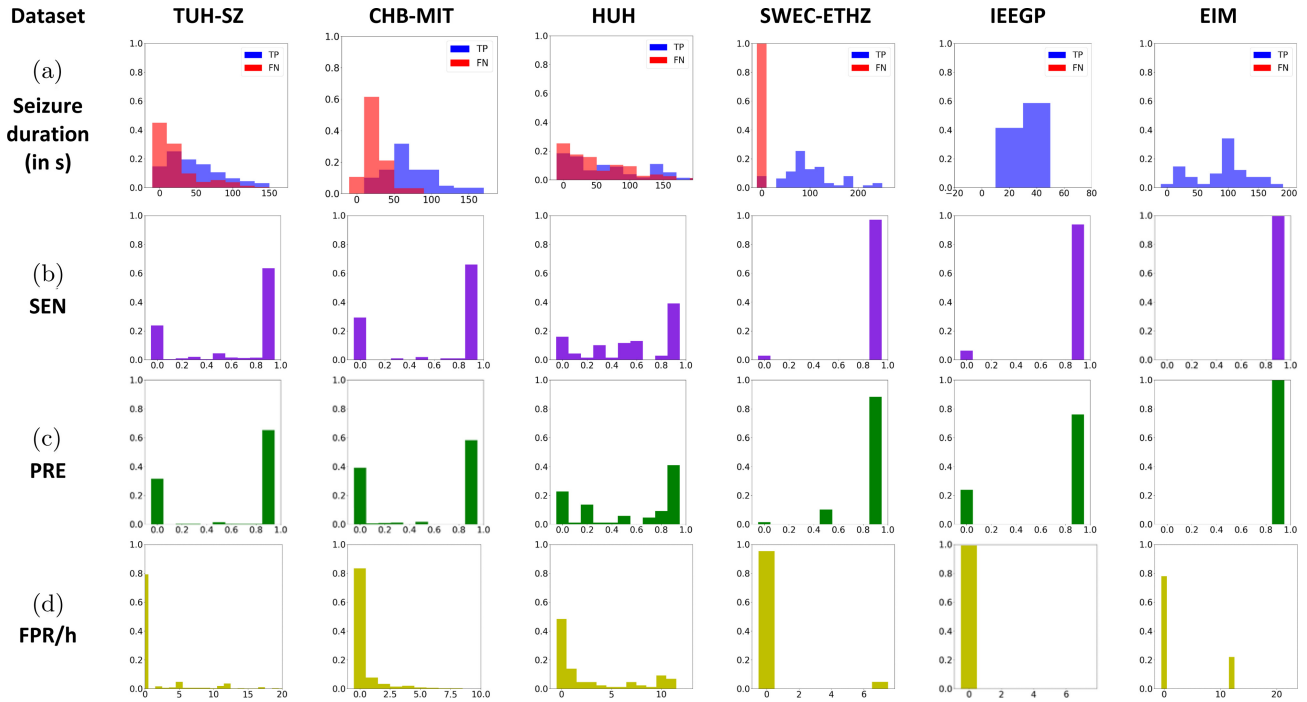


Fig. 4. EEG-level seizure detection results for the CNN-TRF-BM model across different datasets. (a) Normalized histograms of TPs and FNs sorted by seizure duration; (b-d) Normalized histograms of the SEN, PRE, and false positive rate per hour (FPR/h) for individual EEGs, respectively.

detection. In addition, the datasets considered in the literature vary in terms of patients (age, type, diversity), clinical settings, EEG type, data quantity and quality, and use case (patient-specific versus patient-independent).

It is especially critical to specify the use case, as patient-specific detectors may yield much better performance than a patient-independent detector, but cannot be readily deployed. Therefore, comparing these two types of detectors is meaningless. Consequently, we consider studies that report patient-independent seizure detection results on the six datasets analyzed in this paper.

#### 4.1.1. Detection on the TUH-SZ dataset

Numerous patient-independent seizure detectors have been evaluated on the TUH-SZ dataset. Roy *et al.* utilized different machine learning models and reported a SEN and FPR/h of 0.916 and 137.311.<sup>12</sup> Meanwhile, Shah *et al.* applied an LSTM to detect seizures at the segment-level and obtained SEN between 0.33–0.37 and FPR/h between 1.24–20.8.<sup>10</sup> Ayodele *et al.* trained a VGGNet and evaluated it on 24 EEGs, attaining a SEN, FPR/h, and offset of 0.7835, 0.9, and 2.32s, respectively.<sup>11</sup>

Most results reported are not suitable for clinical application; extremely low SEN or high FPR/h. Additionally, most studies did not report the seizure evaluation metrics. When they do, they utilize EBS and OVLP metrics, which fail to represent the requirements of a seizure detector appropriately. In contrast, the proposed CNN-TRF-BM seizure detector achieved superior results calculated with MOES (SEN, PRE, aFPR/h, and mFPR/h of 0.772, 0.429, 0.425, and 0, respectively), which is suitable for clinical applications. However, to the author’s knowledge, no existing studies have reported the PRE, although it is an essential metric in clinical practice. Moreover, only a few studies reported the offset.

#### 4.1.2. Detection on the CHB-MIT dataset

In the following, we review the results of the CHB-MIT dataset reported in the literature. Furbass *et al.* deployed epileptiform wave sequence (EWS) to classify seizures and obtained a SEN and FPR/h of 0.67 and 0.32, respectively.<sup>13</sup> Gãşmez *et al.* applied a CNN and achieved a SEN,

SPE, and FPR/h of 0.531, 0.931, and 7.8, respectively.<sup>15</sup> Ayodele *et al.* employed the CHB-MIT and TUH-SZ dataset and reported a SEN, FPR/h, and offset of 0.7145, 0.76, and 2.32s, respectively.<sup>11</sup> Mansouri *et al.* trained their detector on the CHB-MIT (19 patients) and the TUH-SZ (24 patients) dataset and evaluated the detector on the CHB-MIT dataset.<sup>14</sup> They attained a SEN, SPE, and FPR/h of 0.83, 0.96, and 8, respectively.

The proposed CNN-TRF-BM model achieves better results on the CHB-MIT dataset, with SEN, PRE, aFPR/h, mFPR/h, and offset of 0.678, 0.377, 0.421, 0.118, and 4.684s, respectively. However, we trained our detector with the TUH-SZ dataset instead of the CHB-MIT dataset. The TUH-SZ dataset contains more seizures (3055 events) compared to CHB-MIT (185 events), giving the model more data to learn from. This shows that training the detector on a different but larger dataset may help improve the performance.

#### 4.1.3. Detection on the SWEC-ETHZ dataset

No existing seizure detectors had been evaluated on the SWEC-ETHZ dataset in a patient-independent manner. Existing studies only performed patient-specific detection on this dataset.<sup>42</sup> The current study can be the baseline for patient-independent seizure detection on the SWEC-ETHZ dataset.

#### 4.1.4. Detection on the HUH dataset

No seizure detectors have so far been evaluated on the HUH dataset in a patient-independent manner. Existing studies only evaluated patient-specific seizure detection.<sup>53</sup> This study is the first to perform patient-independent seizure detection at EEG-level on the HUH dataset. Moreover, we applied a detector trained on adult EEGs to detect seizures in neonatal EEGs and attained promising results. This shows that a detector trained on adult seizures may capture neonatal seizures with a high PRE, despite the substantial age gap. As the model has been trained on adult scalp EEG, it struggles to detect all seizures in neonatal EEGs.

#### 4.1.5. Detection on the IIEEGP dataset

Few studies investigated seizure detection on the IIEEGP dataset. All studies are on patient-specific

seizure detections.<sup>54</sup> Similarly, ACC is a poor metric for an imbalanced dataset. Therefore, the current study can be the baseline for patient-independent seizure detection on the IEEGP dataset.

#### 4.1.6. Detection on the EIM dataset

No earlier studies on seizure detection have been conducted on the EIM dataset. The existing studies aim to predict surgical outcomes.<sup>44</sup> This study is the first to analyze the EIM dataset for patient-independent seizure detection.

## 4.2. Commercial detectors

Several commercial seizure detectors are available in the market, such as Persyst,<sup>55</sup> Encevis,<sup>56</sup> and BESA.<sup>56</sup> Earlier studies by Reus *et al.*<sup>37</sup> and Koren *et al.*<sup>38</sup> have compared the performance of Persyst, Encevis, and BESA. We summarized their findings against the performance of the proposed detector in Table 5. Both studies evaluated the commercial detectors on adult scalp EEG datasets; hence, we focus on the TUH-SZ dataset in this section.

The proposed model outperforms the three commercial detectors in the study conducted by Reus *et al.* by a significant margin. Meanwhile, the proposed system outperforms Persyst and BESA in the study by Koren *et al.*, with Encevis reporting similar results to this study. However, we report MOES, TAES, OVLP, and IMS metric results. In contrast, Reus *et al.* and Koren *et al.* only reported IMS, which is more lenient as they consider a detection correct as long as the detection is within 30 s before the start or after the end of the seizure. Koren *et al.* implemented an altered version of IMS, where the margin is increased to 120 s. These metrics introduced a significant margin of error, which is inappropriate in clinical practice.

Table 5. Performance of commercial seizure detectors against the proposed CNN-TRF-BM detector.

Author	No of Patients	No of Seizures	Duration (in hours)	Metrics	Seizure Detector	SEN	aFPR/h
Reus <i>et al.</i> <sup>37</sup>	283	249	8771	IMS	Persyst 14	0.558	0.071
					Encevis 1.9.2	0.518	0.229
					BESA 2.0	0.430	0.100
Koren <i>et al.</i> <sup>38</sup>	81	790	6900	IMS	Persyst 13	0.816	0.9
					Encevis 1.7	0.778	0.2
					BESA 2.0	0.676	0.7
Current study	637 TUH-SZ	3055	922	MOES	CNN-TRF-BM	0.772	0.425
				OVLP	CNN-TRF-BM	0.775	0.423
				IMS	CNN-TRF-BM	0.797	0.412

## 4.3. Transformer for seizure detection

We identified two studies that apply transformers for seizure detection.<sup>22</sup> However, these systems did not implement a channel-level detector but headed directly to the segment-level. Thus, this study is the first to implement a channel-level seizure detector through transformers.

Bhattacharya *et al.* utilized a transformer for patient-specific seizure detection on the CHB-MIT and IEEGP dataset.<sup>22</sup> For the CHB-MIT and IEEGP datasets, they attained an average SEN of 0.985 and 0.948, and FPR/h of 0.124 and 0, respectively. While they used transformers, there were significant differences in the study performed by Bhattacharya *et al.* as compared to this study. First, we followed a patient-independent approach while they designed a patient-specific detector. Second, the proposed system can detect seizures at the channel-level. In contrast, their systems can only detect seizures at the segment-level. Third, we implemented BM loss while they utilized the SM loss.

## 4.4. Complexity of seizure detectors

Most seizure detectors proposed in the literature do not perform channel-level detection and proceed to segment-level detection directly. The main innovation in those studies lies in improving the deep neural networks used for segment-level classification. These deep neural networks typically contain numerous layers (often 10+) and millions of parameters, which require substantial computational power for training. Moreover, such networks tend to overfit specific datasets, leading to poor generalization. We explore whether deeper models lead to better seizure detection performance.

In Table 6, we list different deep learning systems and provide information about their design and seizure detection performance. These neural networks for seizure detectors contain many layers, ranging between 2 and 709, and contain 7600 to 138 million parameters. The inputs to those models also vary significantly, ranging from 5888 to 228,000 input data points. In contrast, the three proposed seizure detectors only require between 384 to 2560 input data points for window lengths varying from 5 s to 20 s. Moreover, the models contain 7 to 15 layers, with 0.16 to 3.5 million parameters for the CNN

and CNN-TRF models. The input size, number of layers, and parameters for the proposed models are much smaller than for most of the existing models listed in Table 6.

Next, we examined the correlation between model size and performance. The proposed seizure detector models reported higher SEN and lower FPR/h than most models with more parameters and layers. The AUC, ACC, BAC, and F1 were comparable, while the SPE was poorer in our model. However, SPE is only computed in segment-level classification, which is not an EEG-level detection metric. Moreover, the proposed models obtained better AUPRC, SEN, and FPR/h than most existing models with fewer parameters and layers.

Overall, the proposed models outshine models with vastly more parameters, which suggests that designing ever-bigger neural networks for seizure detection may not be a fruitful avenue for research. Instead, alternative pipelines with substantially

fewer parameters may perform comparably to the state of the art or even better. In this study, we demonstrated that by first detecting seizures at individual channels, one could vastly reduce the number of parameters while achieving the same or increased level of performance.

## 5. Conclusions and Future work

This study proposed patient-independent seizure detectors that identify seizures on three EEG scales: channel-, segment- and EEG-level. First, the channel-level detectors detect seizures in single-channel segments through a CNN-based deep learning model. Next, we perform segment-level detection based on statistical features extracted from the channel-level outputs based on different scalp regions. At last, we apply post-processing filters to the segment-level outputs to determine any detected seizures' start and end times.

Table 6. Deep learning models in the literature in terms of complexity and performance.

Author	Model	Layers	Parameters (in millions)	Input size	AUC	AUPRC	ACC	BAC	SEN	SPE	PRE	F1	FPR/h
Asif <i>et al.</i> <sup>57</sup>	SeizureNet	133	45.94	150,528	—	—	—	—	—	—	—	0.896	—
	AlexNet	25	62	51,529	—	—	0.768	—	—	—	—	—	—
	VGG16	41	138	50,176	—	—	0.833	—	—	—	—	—	—
	VGG19	47	138	50,176	—	—	0.818	—	—	—	—	—	—
Raghu <i>et al.</i> <sup>23</sup>	SqueezeNet	68	1.2	51,529	—	—	0.851	—	—	—	—	—	—
	GoogleNet	144	7	50,176	—	—	0.745	—	—	—	—	—	—
	Inceptionv3	316	24	89,401	—	—	0.883	—	—	—	—	—	—
	DenseNet201	709	20	50,176	—	—	0.851	—	—	—	—	—	—
	ResNet18	72	11	50,176	—	—	0.862	—	—	—	—	—	—
	ResNet50	177	23	50,176	—	—	0.862	—	—	—	—	—	—
	ResNet101	347	29.4	50,176	—	—	0.863	—	—	—	—	—	—
Covert <i>et al.</i> <sup>28</sup>	TGCN	30	5.5	415,107	0.926	—	—	0.809	0.648	0.970	—	—	—
Yuan <i>et al.</i> <sup>30</sup>	CNN	4	0.04	17,664	0.957	0.906	0.944	—	—	—	—	0.853	—
Zhou <i>et al.</i> <sup>58</sup>	CNN	3	0.4	5,888	—	—	0.595	0.595	0.618	0.572	—	—	—
Saab <i>et al.</i> <sup>24</sup>	ChronoNet	10	12.7	45,600	0.930	—	—	—	—	—	—	0.770	0.100
Emami <i>et al.</i> <sup>25</sup>	VGG16	41	138	50,176	—	—	—	—	0.740	—	—	—	0.200
Ansari <i>et al.</i> <sup>20</sup>	CNN	23	0.0076	54,000	0.830	—	—	—	0.770	—	—	—	0.900
Gomez <i>et al.</i> <sup>15</sup>	CNN	12	0.314	21,504	—	0.440	0.929	0.731	0.531	0.931	0.514	0.461	7.800
	CNN	7	0.16	384	—	—	—	—	0.713	—	0.490	0.581	0
	CNN	7	0.26	640	—	—	—	—	0.701	—	0.491	0.578	0
Current study	CNN	7	0.52	1,280	—	—	—	—	0.701	—	0.512	0.592	0
	CNN	7	1	2,560	—	—	—	—	0.708	—	0.490	0.579	0
	CNN-TRF	15	2.3	384	—	—	—	—	0.772	—	0.429	0.552	0
Current study	CNN-TRF	15	2.5	640	—	—	—	—	0.653	—	0.476	0.551	0
	CNN-TRF	15	2.8	1,280	—	—	—	—	0.671	—	0.534	0.595	0
	CNN-TRF	15	3.5	2,560	—	—	—	—	0.655	—	0.520	0.580	0



We trained and tested the proposed detectors on the TUH-SZ scalp EEG dataset before evaluating the pretrained detectors on five independent scalp EEG and iEEG datasets. Also, we introduced MOES to address some shortcomings of the existing EEG-level detection metrics. To the author's knowledge, this study is one of the first to incorporate a channel-level detector within the seizure detection system.<sup>32</sup> Moreover, we implemented a pipeline that can detect seizures with any number of electrodes and demonstrated that a channel-level detector is essential for reliable seizure detection and boosting the generalization performance. Finally, the proposed seizure detector is computationally efficient, with a computation time of less than 15 s for a 30 min EEG. Hence, the detector may help accelerate and improve EEG annotation in clinical practice.

However, as the seizure detector is based on deep learning, it is nearly impossible to identify the exact features contributing significantly to the seizure discrimination process. We can perform manual feature extraction before deploying the deep learning models in future work. For instance, we can decompose the time series into different frequency bands via wavelet or Fourier transforms. This way, we may understand the contribution and significance of each frequency component of the EEG signals, yielding significantly more information than by just inputting raw time series signals.

Additionally, we will address the problem of detecting artifacts before seizure detection.<sup>49</sup> The artifact detector will be designed to reduce FPR/h and improve the PRE of the seizure detector. Consequently, it can reject artifacts without eliminating important cerebral signals, such as slow waves, sharp waves, and seizures in EEGs.

## References

1. V. K. Jirsa, W. C. Stacey, P. P. Quilichini, A. I. Ivanov and C. Bernard, On the nature of seizure dynamics, *Brain* **137**(8) (2014) 2210–2230.
2. V. D. Nunes, L. Sawyer, J. Neilson, G. Sarri and J. H. Cross, Diagnosis and management of the epilepsies in adults and children: Summary of updated nice guidance, *BMJ* **344** (2012).
3. S. Jenssen, E. J. Gracely and M. R. Sperling, How long do most seizures last? A systematic comparison of seizures recorded in the epilepsy monitoring unit, *Epilepsia* **47**(9) (2006) 1499–1503.
4. M. M. Goldenberg, Overview of drugs used for epilepsy and seizures: Etiology, diagnosis, and treatment, *Pharm. Ther.* **35**(7) (2010) 392.
5. World Health Organization, Programme for Neurological Diseases and Neuroscience (World Health Organization), International Bureau for Epilepsy, International League against Epilepsy, *Atlas: Epilepsy Care in the World* (World Health Organization, 2005).
6. F. F. Ferri, *Ferri's Clinical Advisor 2020*, E-Book: 5 Books in 1 (Elsevier Health Sciences, 2019).\*\*
7. A. T. Berg, Risk of recurrence after a first unprovoked seizure, *Epilepsia* **49** (2008) 13–18.
8. F. Mormann, R. G. Andrzejak, C. E. Elger and K. Lehnertz, Seizure prediction: The long and winding road, *Brain* **130**(2) (2007) 314–333.
9. I. Geut, S. Weenink, I. Knottnerus and M. J. van Putten, Detecting interictal discharges in first seizure patients: Ambulatory EEG or EEG after sleep deprivation? *Seizure* **51** (2017) 52–54.
10. V. Shah, M. Golmohammadi, S. Ziyabari, E. Von Weltin, I. Obeid and J. Picone, Optimizing channel selection for seizure detection, in *2017 IEEE Signal Processing in Medicine and Biology Symposium (SPMB)* (IEEE, 2017), pp. 1–5.
11. K. Ayodele, W. Ikezogwo, M. Komolafe and P. Ogunbona, Supervised domain generalization for integration of disparate scalp EEG datasets for automatic epileptic seizure detection, *Comput. Biol. Med.* **120** (2020) 103757.
12. S. Roy *et al.*, Evaluation of artificial intelligence systems for assisting neurologists with fast and accurate annotations of scalp electroencephalography data, *EBioMedicine* (2021) 103275.
13. F. Furbass *et al.*, Prospective multi-center study of an automatic online seizure detection system for epilepsy monitoring units, *Clin. Neurophysiol.* **126**(6) (2015) 1124–1131.
14. A. Mansouri, S. P. Singh and K. Sayood, Online EEG seizure detection and localization, *Algorithms* **12**(9) (2019) 176.
15. C. Gómez, P. Arbeláez, M. Navarrete, C. Alvarado-Rojas, M. Le Van Quyen and M. Valderrama, Automatic seizure detection based on imaged-EEG signals through fully convolutional networks, *Sci. Rep.* **10**(1) (2020) 1–13.
16. O. Faust, U. R. Acharya, H. Adeli and A. Adeli, Wavelet-based EEG processing for computer-aided seizure detection and epilepsy diagnosis, *Seizure* **26** (2015) 56–64.
17. H. Adeli, Z. Zhou and N. Dadmehr, Analysis of EEG records in an epileptic patient using wavelet transform, *J. Neurosci. Meth.* **123**(1) (2003) 69–87.
18. S. Ghosh-Dastidar, H. Adeli and N. Dadmehr, Mixed-band wavelet-chaos-neural network methodology for epilepsy and epileptic seizure detection, *IEEE Trans. Biomed. Eng.* **54**(9) (2007) 1545–1551.

19. M. Savadkoobi, T. Oladunni and L. Thompson, A machine learning approach to epileptic seizure prediction using electroencephalogram (EEG) signal, *Biocybern. Biomed. Eng.* **40**(3) (2020) 1328–1341.
20. A. H. Ansari, P. J. Cherian, A. Caicedo, G. Naulaers, M. De Vos and S. Van Huffel, Neonatal seizure detection using deep convolutional neural networks, *Int. J. Neural Syst.* **29**(4) (2019) 1850011.
21. X. Hu, S. Yuan, F. Xu, Y. Leng, K. Yuan and Q. Yuan, Scalp EEG classification using deep BiLSTM network for seizure detection, *Comput. Biol. Med.* **124** (2020) 103919.
22. A. Bhattacharya, T. Baweja and S. Karri, Epileptic seizure prediction using deep transformer model, *Int. J. Neural Syst.* (2021) 2150058.
23. S. Raghu, N. Sriraam, Y. Temel, S. V. Rao and P. L. Kubben, EEG based multi-class seizure type classification using convolutional neural network and transfer learning, *Neural Netw.* **124** (2020) 202–212.
24. K. Saab, J. Dunnmon, C. Ré, D. Rubin and C. Lee-Messer, Weak supervision as an efficient approach for automated seizure detection in electroencephalography, *NPJ Digit. Med.* **3**(1) (2020) 1–12.
25. A. Emami, N. Kunii, T. Matsuo, T. Shinozaki, K. Kawai and H. Takahashi, Seizure detection by convolutional neural network-based analysis of scalp electroencephalography plot images, *NeuroImage: Clin.* **22** (2019) 101684.
26. H. S. Nogay and H. Adeli, Detection of epileptic seizure using pretrained deep convolutional neural network and transfer learning, *Eur. Neurol.* **83**(6) (2020) 602–614.
27. S. Santaniello, S. P. Burns, A. J. Golby, J. M. Singer, W. S. Anderson and S. V. Sarma, Quickest detection of drug-resistant seizures: An optimal control approach, *Epilepsy Behav.* **22** (2011) S49–S60.
28. I. C. Covert, B. Krishnan, I. Najm, J. Zhan, M. Shore, J. Hixson and M. J. Po, Temporal graph convolutional networks for automatic seizure detection, in *Proceedings of the 4th Machine Learning for Healthcare Conference* (Ann Arbor, Michigan, 2019), pp. 160–180.
29. S. Roy, I. Kiral-Kornek and S. Harrer, Chrononet: A deep recurrent neural network for abnormal EEG identification, in *Conf. Artificial Intelligence in Medicine in Europe* (Springer, 2019), pp. 47–56.
30. Y. Yuan, G. Xun, K. Jia and A. Zhang, A multi-view deep learning framework for EEG seizure detection, *IEEE J. Biomed. Health Inf.* **23**(1) (2018) 83–94.
31. C. Guo, G. Pleiss, Y. Sun and K. Q. Weinberger, On calibration of modern neural networks, in *Proceedings of the 34th International Conference on Machine Learning* (International Convention Centre, Sydney, Australia, 2017), pp. 1321–1330.
32. Y. Lu, Y. Ma, C. Chen and Y. Wang, Classification of single-channel EEG signals for epileptic seizures detection based on hybrid features, *Technol. Health Care* **26**(S1) (2018) 337–346.
33. U. R. Acharya, S. L. Oh, Y. Hagiwara, J. H. Tan and H. Adeli, Deep convolutional neural network for the automated detection and diagnosis of seizure using EEG signals, *Comput. Biol. Med.* **100** (2018) 270–278.
34. G. Liu, L. Tian and W. Zhou, Patient-independent seizure detection based on channel-perturbation convolutional neural network and bidirectional long short-term memory, *Int. J. Neural Syst.* **32**(6) (2022) 2150051.
35. L. Spyrou, D. Martín-Lopez, A. Valentín, G. Alarcón and S. Sanei, Detection of intracranial signatures of interictal epileptiform discharges from concurrent scalp EEG, *Int. J. Neural Syst.* **26**(4) (2016) 1650016.
36. V. Shah, M. Golmohammadi, I. Obeid and J. Picone, Objective evaluation metrics for automatic classification of EEG events, *Biomed. Signal Process.* (2021) 223–255.
37. E. Reus, G. Visser, J. van Dijk and F. Cox, Automated seizure detection in an EMU setting: Are software packages ready for implementation? *Seizure* **96** (2022) 13–17.
38. J. Koren, S. Hafner, M. Feigl and C. Baumgartner, Systematic analysis and comparison of commercial seizure-detection software, *Epilepsia* **62**(2) (2021) 426–438.
39. V. Shah, E. Von Weltin, S. Lopez, J. R. McHugh, L. Veloso, M. Golmohammadi, I. Obeid and J. Picone, The temple university hospital seizure detection corpus, *Front. Neuroinform.* **12** (2018) 83.
40. A. Shoeb, H. Edwards, J. Connolly, B. Bourgeois, S. T. Treves and J. Guttag, Patient-specific seizure onset detection, *Epilepsy Behav.* **5**(4) (2004) 483–498.
41. N. Stevenson, K. Tapani, L. Lauronen and S. Vanhatalo, A dataset of neonatal EEG recordings with seizure annotations, *Sci. Data* **6**(1) (2019) 1–8.
42. A. Burrello, K. Schindler, L. Benini and A. Rahimi, Hyperdimensional computing with local binary patterns: One-shot learning of seizure onset and identification of ictogenic brain regions using short-time ieeeg recordings, *IEEE Trans. Biomed. Eng.* **67**(2) (2019) 601–613.
43. J. B. Wagenaar, B. H. Brinkmann, Z. Ives, G. A. Worrell and B. Litt, A multimodal platform for cloud-based collaborative research, in *2013 6th Int. IEEE/EMBS Conf. Neural Engineering (NER)* (IEEE, 2013), pp. 1386–1389.
44. A. Li et al., Neural fragility as an EEG marker of the seizure onset zone, *Nat. Neurosci.* **24**(10) (2021) 1465–1474.
45. J. Thomas et al., Automated adult epilepsy diagnostic tool based on interictal scalp electroencephalogram characteristics: A six-center study, *Int. J. Neural Syst.* (2021) 2050074.
46. P. Thangavel et al., Time-frequency decomposition of scalp electroencephalograms improves deep

- learning-based epilepsy diagnosis, *Int. J. Neural Syst.* (2021) 2150032.
47. W. Y. Peh *et al.*, Multi-center validation study of automated classification of pathological slowing in adult scalp electroencephalograms via frequency features, *Int. J. Neural Syst.* (2021) 2150016.
  48. T. Joo, U. Chung and M.-G. Seo, Being bayesian about categorical probability, in *Proc. 37th Int. Conf. Machine Learning* (Virtual, 2020), pp. 4950–4961.
  49. W. Y. Peh, Y. Yao and J. Dauwels, Transformer convolutional neural networks for automated artifact detection in scalp EEG, in *2022 44th Annual Int. Conf. IEEE Engineering in Medicine and Biology Society (EMBC)* (IEEE, 2022), pp. 3599–3602.
  50. C.-S. Ouyang, R.-C. Yang, R.-C. Wu, C.-T. Chiang and L.-C. Lin, Determination of antiepileptic drugs withdrawal through EEG hjorth parameter analysis, *Int. J. Neural Syst.* **30**(11) (2020) 2050036.
  51. P. Afra, C. C. Jouny and G. K. Bergey, Duration of complex partial seizures: An intracranial EEG study, *Epilepsia* **49**(4) (2008) 677–684.
  52. M. J. Cook *et al.*, Prediction of seizure likelihood with a long-term, implanted seizure advisory system in patients with drug-resistant epilepsy: A first-in-man study, *Lancet Neurol.* **12**(6) (2013) 563–571.
  53. A. O’Shea, G. Lightbody, G. Boylan and A. Temko, Neonatal seizure detection from raw multi-channel EEG using a fully convolutional architecture, *Neural Netw.* **123** (2020) 12–25.
  54. B. H. Brinkmann *et al.*, Crowdsourcing reproducible seizure forecasting in human and canine epilepsy, *Brain* **139**(6) (2016) 1713–1722.
  55. A. Sierra-Marcos, M. L. Scheuer and A. O. Rossetti, Seizure detection with automated EEG analysis: A validation study focusing on periodic patterns, *Clin. Neurophysiol.* **126**(3) (2015) 456–462.
  56. N. Rommens, E. Geertsema, L. J. Holleboom, F. Cox and G. Visser, Improving staff response to seizures on the epilepsy monitoring unit with online EEG seizure detection algorithms, *Epilepsy Behav.* **84** (2018) 99–104.
  57. U. Asif, S. Roy, J. Tang and S. Harrer, SeizureNet: Multi-spectral deep feature learning for seizure type classification, *Mach. Learn. Clin. Neuroimaging Radiogenomics Neurooncology* (2020) 77–87.
  58. M. Zhou, C. Tian, R. Cao, B. Wang, Y. Niu, T. Hu, H. Guo and J. Xiang, Epileptic seizure detection based on EEG signals and CNN, *Front. Neuroinform.* **12** (2018) 95.